JOURNAL OF VIROLOGY, Dec. 1979, p. 812-821
0022-538X/79/12-0812/10$02.00/0

Vol. 32, No. 3

Analysis of the DNAs from Seven Varicella-Zoster Virus Isolates

JAMES C. RICHARDS, RICHARD W. HYMAN,* AND FRED RAPP

Department of Microbiology and Specialized Cancer Research Center, The Pennsylvania State University College of Medicine, Hershey, Pennsylvania 17033

Received for publication 7 June 1979

The ^{32}P-labeled DNAs from seven different clinical isolates of human varicella-zoster virus (VZV) were independently digested with five site-specific restriction endonucleases, *Eco*RI, *Hin*dIII, *Sma*I, *Bam*HI, and *Ava*I. The digestion products were analyzed by electrophoresis on 0.5% agarose gels followed by autoradiography of the dried gels. Evaluation of the restriction enzyme cleavage patterns revealed small variations among the VZV DNAs. The VZV DNAs were also compared based on their buoyant densities in CsCl. No significant buoyant density differences were detected among the VZV DNAs.

Varicella-zoster virus (VZV) is the causative agent of chickenpox (varicella) and shingles (herpes zoster) in humans (26). VZV infection of human embryo fibroblast cells in culture results in a characteristic focal cytopathological reaction in which the virus remains cell associated. Since isolation of VZV DNA from purified virions is inefficient, we used a version of the Hirt procedure for VZV DNA isolation (12, 20). In previous publications, we reported that the *Eco*RI and *Hin*dIII restriction patterns of the DNAs from five VZV isolates were indistinguishable (19) and that the CsCl buoyant densities of the VZV DNAs showed slight variations among the isolates (13). In the present communication, we examined the DNAs of three of the previous VZV isolates and four new VZV isolates with respect to variation in restriction endonuclease cleavage patterns and CsCl buoyant densities. Several important improvements have been made in the experimental techniques. For restriction enzyme cleavage analysis, horizontal gels were used instead of vertical gels because of greater stability. X-ray intensifying screens were used to enhance autoradiography (24). For CsCl buoyant density analyses, artificial mixtures of [^{3}H]thymidine ([^{3}H]TdR)- and [^{14}C]TdR-labeled herpes simplex virus (HSV) DNAs were added to each gradient as internal controls for isotope effects (6). In this context, the term "isotope effect" refers to a change in buoyant density solely due to a change in mass because ^{14}C is inherently heavier than ^{12}C. Based on these improvements in technique and the use of new VZV isolates, we now report differences among VZV DNAs on the basis of their restriction endonuclease cleavage patterns. The slight differences in CsCl buoyant density found among the VZV DNAs were not more than can be ascribed to the isotope effect.

MATERIALS AND METHODS

Cells and virus stocks. Flow 5000 cells (Flow Laboratories, Inc., Rockville, Md.) were propagated at 37°C in Dulbecco medium containing 10% fetal calf serum with 0.075% $NaHCO_3$. The VZV isolates used in this study are presented in Table 1. VZV (Ma) and (Rc) were generously provided by L. Rasmussen, Stanford University Medical Center, Stanford, Calif. VZV (Ma) was isolated from a 7-year-old female with fatal generalized varicella and an underlying nucleoside phosphorylase deficiency disease. VZV (Rc) was isolated from a 9-year-old female with generalized varicella and acute lymphocytic leukemia. VZV (Caufield), (Ludwig), and (Jab) were obtained in Hershey, Pa. VZV (Kawaguchi) and (Oka) were generously provided by M. Takahashi (1, 25).

Radioactive labeling and purification of VZV DNA. ^{32}P-labeled VZV DNA was prepared as follows. Twelve hours after mixing VZV-infected and uninfected cells at an infected-to-uninfected cell ratio of 1:3 in T-75 or T-150 flasks (Falcon Plastics, Oxnard, Calif.), the medium was decanted, and 15 ml of phosphate-free minimal essential medium containing 2% dialyzed fetal calf serum, 100 μCi of [^{32}P]P_i per ml (New England Nuclear, Boston, Mass.), and 0.5 μCi of [^{3}H]TdR per ml (40 to 60 Ci/mmol, New England Nuclear) was added. The infection was allowed to progress for 24 to 36 h or until the cytopathic effect was greater than 80%. The VZV [^{32}P]DNA was then purified as described (13, 19, 20). VZV DNA from the peak fractions of the glycerol gradient was dialyzed against two changes of 0.01 M Tris (pH 8.0)-0.001 M EDTA (TE buffer) overnight at 4°C. The VZV DNA was concentrated to about 5 ml by dialysis against Aquacide (Calbiochem, La Jolla, Calif.). The VZV DNA was deproteinized by treatment with Proteinase K (100 μg/ml) for 2 h at 37°C, extracted with phenol (saturated with TE buffer), and then extracted with

TABLE 1. *Sources and passage numbers of VZV isolates*

VZV isolate	Origin	Source	Passage no.	
			Restriction enzyme cleavage	Buoyant density
(Ma)	VSV-infected skin biopsy	L. Rasmussen, Stanford Univ. Medical Center, Calif.	10	14
(Rc)	Vesicular fluid from child with chickenpox	L. Rasmussen, Stanford Univ. Medical Center, Calif.	9	13
(Kawaguchi)	Vesicular fluid from child with chickenpox	M. Takahashi, Osaka Univ., Japan	47	48
(Oka)	Vesicular fluid from child with chickenpox	M. Takahashi, Osaka Univ., Japan	18	18
(Caufield)	Vesicular fluid from adult with herpes zoster	Hershey Medical Center, Hershey, Pa.	13	14
(Ludwig)	Vesicular fluid from adult with herpes zoster	Hershey Medical Center, Hershey, Pa.	36	40
(Jab)	Vesicular fluid from adult with herpes zoster	Hershey Medical Center, Hershey, Pa.	23	14

chloroform–isoamyl alcohol (24:1). The VZV DNA, in the aqueous phase, was precipitated by ethanol, dissolved in TE buffer, and centrifuged twice to equilibrium in CsCl buoyant density gradients. ^{32}P-labeled HSV type 1 (HSV-1) strains KOS and Patton and HSV type 2 (HSV-2) strain 333 DNAs, prepared essentially as described (19), routinely had specific activities of 0.5×10^6 to 1.0×10^6 cpm/μg. [^{3}H]TdR and [^{14}C]TdR labeling of VZV and HSV DNAs was accomplished by including either [^{3}H]TdR at 10 μCi/ml (40 to 60 Ci/mmol) or [^{14}C]TdR at 1 μCi/ml (40 to 60 mCi/mmol) in the medium (13, 15).

Endonuclease digestion and gel electrophoresis. All restriction endonucleases were purchased from New England Biolabs (Beverly, Mass.) and were used essentially as described by the manufacturer. The DNA sample (2×10^4 cpm), 0.002 ml of 10× salts, water, and the specific enzyme (5- to 10-fold enzyme excess) were added together to yield a final volume of 0.020 ml. The reaction vessels were sealed and incubated at 37°C for 2 h. Reactions were terminated by adding 0.005 ml of loading buffer (30% [wt/vol] Ficoll–0.06 M EDTA–0.5% [wt/vol] sodium dodecyl sulfate–0.2% [wt/vol] bromophenol blue–0.25 M Tris [pH 8.0]). The samples were mixed gently, heated at 55°C for 3 to 5 min, and centrifuged at $50 \times g$ for 1 min to concentrate all material into the bottom of the reaction tube. Samples were loaded into preformed slots on a 0.5% horizontal agarose slab gel (18).

Electrophoresis-grade agarose (BioRad Laboratories, Richmond, Calif.) was prepared in E buffer (0.04 M Tris base–0.005 M sodium acetate–0.001 M EDTA, adjusted to pH 7.9 with glacial acetic acid) (21). Electrophoresis was conducted at 3.2 V/cm for 14 h at 22°C. Gels were dried on Whatman 3-mm filter paper, placed in contact with Kodak RPX-omat R or L film, and sandwiched between two Cronex intensifying screens (E. I. duPont de Nemours, Wilmington, Del.). Photoscans of autoradiographs were made using a Transidyne 2955 scanning densitometer with computing integrator capability.

RESULTS

Comparison of VZV DNAs by CsCl buoyant density centrifugation. [^{3}H]TdR DNA and [^{14}C]TdR DNA were prepared for each of the seven VZV isolates. All 49 possible twofold comparisons of the buoyant densities of these VZV DNAs in CsCl were accomplished. As internal controls for isotope effect, HSV [^{3}H]TdR DNA and HSV [^{14}C]TdR DNA were included in each gradient. In each case, the HSV DNAs had a density of 1.727 g/cm^3. Only representative CsCl gradients will be shown. The buoyant densities of VZV DNAs of the varicella isolates were compared (data not shown); no significant differences were observed. Comparisons of the buoyant densities of ^{14}C- and ^{3}H-labeled VZV DNAs from herpes zoster isolates were made (data not shown); no significant differences were observed. The final part of the buoyant density studies was a comparison of VZV DNA from the varicella isolates with VZV DNA from the herpes zoster isolates. Figure 1 shows that the ^{14}C-labeled DNA had the slightly greater buoyant density. The buoyant density difference between VZV [^{14}C]DNA and VZV [^{3}H]DNA was never greater than the density difference observed between HSV [^{14}C]DNA and HSV [^{3}H]-DNA within the same gradients (Fig. 1a, f, g, and h). Thus, we conclude from all these buoyant density measurements (Fig. 1 and other data not shown) that the observed slight differences in the CsCl buoyant densities for VZV DNAs were not larger than can be accounted for by the isotope effect, and that therefore the CsCl buoyant density of VZV DNA is indistinguishable for all clinical isolates.

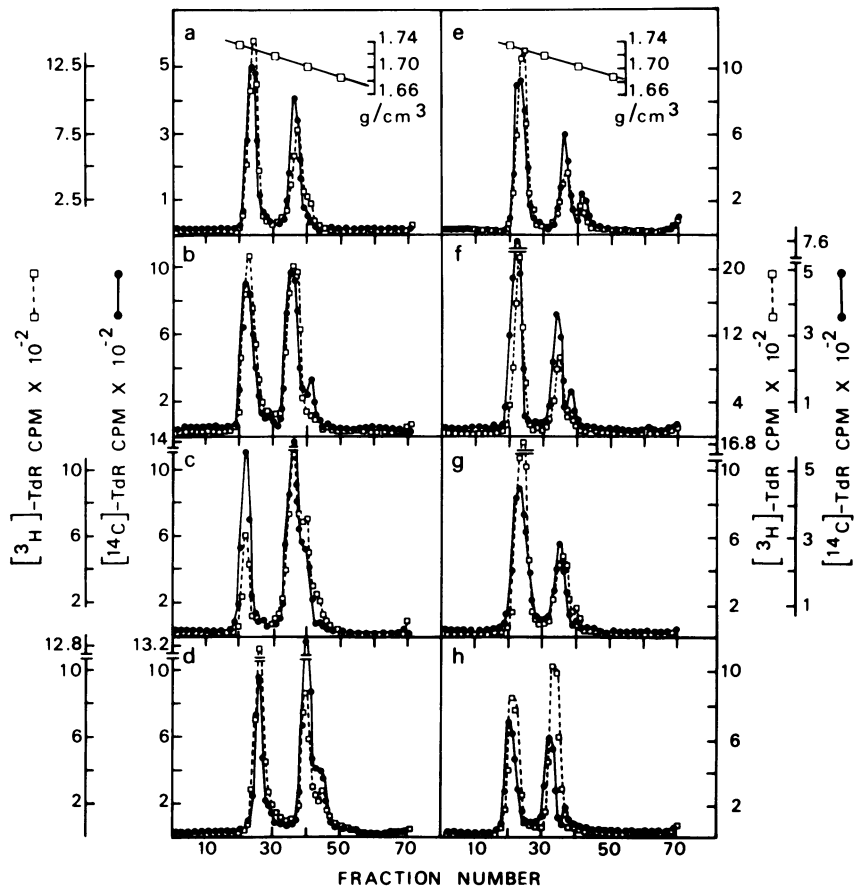

FIG. 1. *CsCl buoyant density analysis of VZV DNAs. VZVs isolated from clinical infections were propagated in Flow 5000 cells and independently labeled with [^{3}H]TdR or [^{14}C]TdR, and the VZV DNAs were purified as described (13, 19, 20). Flow 5000 cells, infected with HSV-1 (KOS) at a multiplicity of infection of 5, were labeled with either [^{14}C]- or [^{3}H]TdR, and HSV DNA was purified from the Hirt supernatant of infected cells by CsCl density gradient centrifugation. All gradient analyses represent artificial mixtures of ^{3}H-labeled and ^{14}C-labeled VZV DNAs, radiolabeled and purified before these reconstitution measurements. HSV-1 (KOS) [^{14}C]- and [^{3}H]TdR DNAs were included in all reconstitution experiments as an internal control for isotope effect and, in each panel, are the DNAs of density 1.727 g/cm^3 (the left-most bands). The total mass of DNA in each gradient never exceeded 2 μg. Isopycnic centrifugation was carried out at 35,000 rpm for 65 h at 20°C in a Beckman 50.3 rotor. Gradients were fractionated from the bottom by pumping. Volumes of each fraction were precipitated on filter disks and counted in a liquid scintillation counter. The refractive index of certain fractions was measured. Using standard tables, refractive index was converted to density. To avoid cluttering the figure, the density values are plotted only for the gradient at the top of each column. Density increases from right to left. A small amount of contaminating cell DNA is seen as the lightest (shoulder) DNA for [^{3}H]DNA in panels a, c, d, e, and g and for [^{14}C]DNA in panels b, c, d, e, f, and h. (a) VZV (Jab) [^{3}H]DNA and VZV (Oka) [^{14}C]DNA; (b) VZV (Oka) [^{3}H]DNA and VZV (Jab) [^{14}C]DNA; (c) VZV (Ludwig) [^{3}H]DNA and VZV (Oka) [^{14}C]DNA; (d) VZV (Oka) [^{3}H]DNA and VZV (Ludwig) [^{14}C]DNA; (e) VZV (Caufield) [^{3}H]DNA and VZV (Ma) [^{14}C]DNA; (f) VZV (Ma) [^{3}H]DNA and VZV (Caufield) [^{14}C]DNA; (g) VZV (Caufield) [^{3}H]DNA and VZV (Kawaguchi) [^{14}C]DNA; (h) VZV (Kawaguchi) [^{3}H]DNA and VZV (Caufield) [^{14}C]DNA. Symbols: ●, ^{14}C counts per minute; □, ^{3}H counts per minute.*

The buoyant density in CsCl of all seven VZV DNAs was 1.705 g/cm^3, as determined both by refractive index measurements and interpolations based on the gradient positions of HSV-1 DNA (density of 1.727 g/cm^3) (14) and cell DNA (density of 1.695 g/cm^3). This value is in agreement with the values published by Ludwig et al. (17) and Iltis et al. (13).

Analysis of *Eco*RI-generated VZV DNA fragments. Molecular weight standards (restriction enzyme-cleaved HSV DNA) were included in all gels in at least two different posi-

tions to account for possible discontinuities within the horizontal slab gel. As a control, uncleaved VZV DNA was also electrophoresed in all gels (data not shown). The uncut VZV DNA always migrated as a single, broad band with a slower mobility than all the restriction endonuclease-derived bands. To save space, usually only one set of molecular weight standards is shown in each figure. Plots of distance migrated versus log molecular weight for HSV DNA fragment markers were linear between 1 and 10 megadaltons (Mdal) in all gels analyzed (data not shown).

VZV DNAs from each of the seven VZV clinical isolates were individually digested by restriction endonuclease *Eco*RI. The specific DNA fragments were separated by electrophoresis on an agarose gel. The *Eco*RI-generated VZV DNA fragments are shown in Fig. 2. The molecular weight standards were HSV-1 (KOS) DNA digested by *Eco*RI (Fig. 2, track 1) and by *Hin*dIII (Fig. 2, track 8). The *Eco*RI cleavage patterns of VZV (Kawaguchi) (Fig. 2, track 4), (Oka) (Fig. 2, track 5), and (Jab) (Fig. 2, track 7) DNAs were indistinguishable from our previously published patterns (19) with the exception of the low-molecular-weight bands (M, N, O, and P), which are now visualized by use of intensifying screens. The single most important point in Fig. 2 was that the *Eco*RI cleavage patterns for VZV DNAs were obviously very similar for all seven isolates (Fig. 2, tracks 2 to 7). The *Eco*RI cleavage pattern of VZV (Caufield) DNA was indistinguishable from the pattern of VZV (Oka) DNA (data not shown). The VZV (Rc) DNA cleavage pattern (Fig. 2, track 2) showed the most variation compared to the cleavage patterns of the other VZV DNAs (Fig. 2, tracks 3 to 7). This observation is attributed to the presence of the A1 fragment (Fig. 2, track 2) and the absence of the B and E fragments for *Eco*RI-cleaved VZV (Rc) DNA. These patterns were confirmed by two independent DNA preparations for each VZV isolate as well as by electrophoresis on 0.3% agarose gels. The designation of infrequently appearing bands in the cleavage patterns was by capital letters followed by a number. The infrequently observed bands in the *Eco*RI cleavage patterns of VZV DNAs were the A1 band of VZV (Rc) DNA, the F1 band of VZV (Oka) DNA, and the H1 bands of VZV (Oka), (Ludwig), and (Jab) DNAs (Fig. 2, tracks 2, 5, 6, and 7, respectively).

For quantitation of the *Eco*RI cleavage patterns of VZV DNA, autoradiographs such as Fig. 2 were first scanned with a densitometer. To save space, the densitometer scans will not be shown. Quantitative analysis of the [^{32}P]DNA content within each restriction fragment, derived from both automatic and graphic integration of densitometer scans, revealed both molar and submolar fragments (Table 2). The calculated relative molar yields among comigrating fragments of *Eco*RI-cleaved VZV DNAs were very similar, again reflecting homogeneity among the VZV isolates (Table 2). The molecular weights of the *Eco*RI-generated VZV DNA fragments ranged from 11 to 0.40 Mdal for VZV (Ma), (Kawaguchi), (Oka), (Caufield), (Ludwig), and (Jab) DNAs (Table 2). The VZV (Rc) DNA fragments ranged from 25 to 0.40 Mdal (Table 2). Because the relative molar yields cannot be interpreted unambiguously in terms of a model for the organization of the VZV genome (see Discussion), the calculation of relative molar yield is presented only for the *Eco*RI-digested VZV DNA and not for the subsequent restriction enzyme digestions.

Analysis of *Hin*dIII-generated VZV DNA fragments. The DNAs from the seven VZV isolates were individually cleaved with *Hin*dIII and analyzed by electrophoresis on 0.5% agarose gels. Improved experimental procedures allowed a substantial improvement in the technical quality of these patterns compared to our previously published patterns (19). The autoradiographs of the *Hin*dIII cleavage pattern (Fig. 3) indicate a high degree of similarity among the DNAs of the seven VZV isolates. Based on the *Hin*dIII cleavage patterns, three qualitatively distinguishable groups are present among the seven VZV DNAs examined. The most frequently observed *Hin*dIII cleavage pattern of VZV DNA was indistinguishable for VZV (Kawaguchi), (Caufield), (Ma), and (Rc) DNAs and is shown for VZV (Ma) and (Rc) DNAs in Fig. 3 (tracks 2 and 3, respectively). The second *Hin*dIII cleavage pattern was observed for VZV (Ludwig) and (Jab) DNAs (Fig. 3, tracks 5 and 6, respectively). The VZV (Ludwig) and (Jab) DNA pattern differs from the VZV (Ma), (Rc), (Kawaguchi), and (Caufield) DNA pattern by the presence of 6.2-Mdal fragment D in the former and not in the latter (Fig. 3, tracks 5 and 6, cf. tracks 2 and 3). VZV (Oka) DNA possessed the third *Hin*dIII cleavage pattern which was distinguishable from all the others by the presence of band D and absence of band E (Fig. 3, track 4). The *Hin*dIII fragments of VZV DNAs ranged in molecular weight from 13 to 0.9 Mdal and comprised both molar and submolar populations (Table 3).

Analysis of *Sma*I-generated VZV DNA fragments. DNAs from each VZV isolate were individually digested with *Sma*I, and the resulting fragments were separated by electrophoresis on 0.5% agarose gels. Autoradiography of the

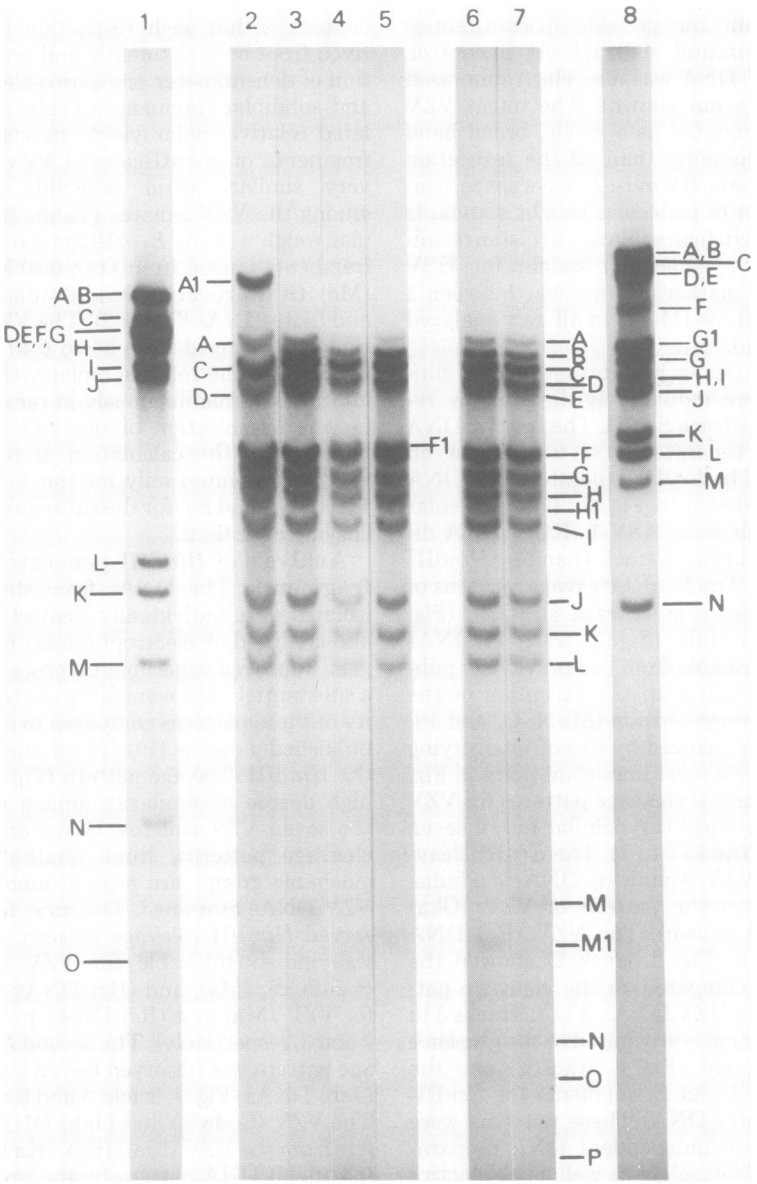

FIG. 2. *Autoradiographs showing the EcoRI digestion patterns of VZV DNAs. The seven VZV DNAs were each radiolabeled in vivo with [^{32}P]P$_i$ and purified from the Hirt supernatant as described (13, 19, 20). Each VZV DNA was digested by EcoRI. After electrophoresis of the cleavage fragments on a 0.5% agarose gel, the gel was dried and autoradiography was performed. Variously exposed autoradiographs are combined to achieve comparable contrast among the samples. The nomenclature for the restriction enzyme cleavage fragments of VZV DNA follows the convention adopted for HSV DNA: the specific DNA fragments are designated by capital letters of the alphabet in order of increasing electrophoretic mobility (decreasing size). An infrequently appearing fragment of VZV DNA is designated by the letter of the analogous frequently appearing fragment followed by the number 1. (Track 1) HSV-1 (KOS) DNA cleaved by EcoRI. This pattern is indistinguishable from the pattern published by Skare and Summers (22) and uses their nomenclature. (Track 2) VZV (Rc) DNA cleaved by EcoRI. (Track 3) VZV (Ma) DNA cleaved by EcoRI. (Track 4) VZV (Kawaguchi) DNA cleaved by EcoRI. (Track 5) VZV (Oka) DNA cleaved by EcoRI. The EcoRI cleavage pattern of VZV (Caufield) DNA was identical to the EcoRI cleavage pattern of VZV (Oka) DNA and, to save space, is not shown. (Track 6) VZV (Ludwig) DNA cleaved by EcoRI. (Track 7) VZV (Jab) DNA cleaved by EcoRI. (Track 8) HSV-1 (KOS) DNA cleaved by HindIII. This HindIII cleavage pattern of HSV-1 DNA is indistinguishable from the analogous pattern for HSV-1 (strain 17) DNA published by Wilkie (28), with the exceptions of the additional presence of band G1 and the absence of band 0.*

TABLE 2. *Molecular weights and relative molar yields of VZV DNA fragments generated by EcoRI digestion*[a]

Fragment designation	Mol wt (Mdal)	Relative molar yield			
		VZV (Ma)[b]	VZV (Rc)	VZV (Oka)[c]	VZV (Jab)[d]
A1	25.0	NP[e]	0.39	NP	NP
A	11.0	0.27	0.29	0.10	0.13
B	10.0	0.59	NP	0.60	0.47
C	9.0	1.70	1.33	1.34	1.23
D	8.1	1.16	0.80	1.07	1.18
E	7.9	0.2	NP	0.1	0.28
F1	6.1	NP	NP	0.51	NP
F	5.9	2.10	2.51	1.57	2.0
G	5.6	1.43	1.55	1.10	1.41
H	5.0	1.1	0.99	0.73	0.91
H1	4.8	NP	NP	0.08	0.08
I	4.6	0.71	0.74	0.73	0.63
J	3.4	1.0	1.0	1.0	1.0
K	2.9	0.80	0.95	0.88	0.92
L	2.7	0.64	0.77	0.78	0.74
M	1.0	0.92	NP	NP	0.81
M1	0.9	NP	0.71	0.86	NP
N	0.58	0.30	0.41	0.43	0.29
O	0.50	0.77	1.05	0.95	0.67
P	0.39	0.45	0.20	0.20	0.30

[a] Band designations are described in the legend to Fig. 2. To calculate the mass in arbitrary units of each band, graphical and automatic integrations were performed for two traces for each of two autoradiographs such as Fig. 2 for each VZV DNA preparation. For the calculation of molar yield relative to band J, the known molecular weights of the bands of the *Eco*RI-cleaved HSV-1 (KOS) DNA (11, 22, 23, 28) and *Hin*dIII-cleaved HSV-1 (KOS) DNA (22, 28) were used to construct a graph of log molecular weight versus distance migrated (data not shown). This curve was linear between 1 and 10 Mdal. Molecular weights outside the linear region must be taken as approximate. The molecular weights of the bands of *Eco*RI-cleaved VZV DNAs were then determined. The mass in arbitrary units for each band was divided by its molecular weight to give the molar yield in arbitrary units. As band J was clearly separated from other bands in the gel (Fig. 2), it was taken as reference. The molar yield in arbitrary units for each band was divided by the molar yield in arbitrary units for band J to give the molar yield relative to band J.

[b] The data for the fragments of VZV (Ma) DNA were also representative of the fragments of VZV (Kawaguchi) DNA with the exceptions of the absence of band M from and the presence of band M1 in the *Eco*RI-digestion pattern of VZV (Kawaguchi) DNA.

[c] The data for the fragments of VZV (Oka) DNA were indistinguishable from the data for VZV (Caufield) DNA, which are, therefore, not shown.

[d] The data for the fragments of VZV (Jab) DNA were representative of the data for the fragments of VZV (Ludwig) DNA, with the exceptions that band M appears only in the *Eco*RI-digestion pattern of VZV (Jab) DNA and band M1 only in the pattern of VZV (Ludwig) DNA.

[e] NP, Not present.

dried gels revealed three distinct cleavage patterns (Fig. 4, tracks 2 to 4). VZV (Rc), (Oka), (Caufield), and (Ludwig) DNAs had indistinguishable *Sma*I cleavage patterns (Fig. 4, track 4). The C and D fragments (Fig. 4) were observed as distinct species after visualization of underexposed autoradiographs. The *Sma*I cleavage patterns for VZV (Ma) and (Jab) DNAs (Fig. 4, tracks 2 and 3, respectively) were distinct. The J1 and P1 fragments (Fig. 4, track 2) were both unique to VZV (Ma) DNA. The P1 and P fragments (Fig. 4) had similar but distinguishable molecular weights. The K1 band in the *Sma*I cleavage pattern of VZV (Ma) DNA (Fig. 4, track 2) was not observed in other digests, although it could be hidden within the K band. The only qualitative difference between patterns for VZV (Jab) and (Ludwig) DNAs was the presence of the H1 band (Fig. 4, track 4) in VZV (Ludwig) DNA. The molecular weights of the *Sma*I fragments of VZV DNA are given in Table 3.

Analysis of *Bam*HI-generated VZV DNA fragments. The seven VZV DNAs were digested with *Bam*HI and subjected to agarose gel electrophoresis. Figure 5 is an autoradiograph of one gel. All the *Bam*HI cleavage patterns of VZV DNAs were subsets of the VZV (Ludwig) DNA pattern (Fig. 5, track 3), differing at most by three bands. The *Bam*HI digestion patterns for VZV (Rc), (Kawaguchi), and (Oka) DNAs were qualitatively indistinguishable from the pattern for VZV (Jab) DNA (Fig. 5, track 4) with the single addition of band F (4.4 Mdal; Table 3). The VZV (Ma) DNA cleavage pattern (Fig. 5, track 2) was indistinguishable from the VZV (Jab) DNA pattern (Fig. 5, track 4) except for the presence of fragment P for VZV (Ma) DNA. The VZV (Ludwig) and (Caufield) DNA patterns were superimposable except for the presence of submolar band C1 for VZV (Ludwig) DNA. The *Bam*HI digestion products of VZV DNA ranged from 8.8 to 0.8 Mdal (Table 3).

Analysis of *Ava*I-generated VZV DNA fragments. The seven VZV DNAs were digested with the restriction endonuclease *Ava*I, and the resulting fragments were separated by agarose gel electrophoresis. Figure 6 is an autoradiograph of one gel. The *Ava*I cleavage patterns of VZV DNAs were indistinguishable with respect to the number and molecular weights of the bands and are represented by the VZV (Ludwig) DNA pattern (Fig. 6, track 2). The *Ava*I enzyme produced VZV DNA fragments which ranged from 8.7 to 0.3 Mdal (Fig. 6). Several very broad DNA bands were observed (Fig. 6, track 2: bands, D, E, G, L, M, and N). These could not be explained on the basis of an overexposed autoradiograph, since very faint expo-

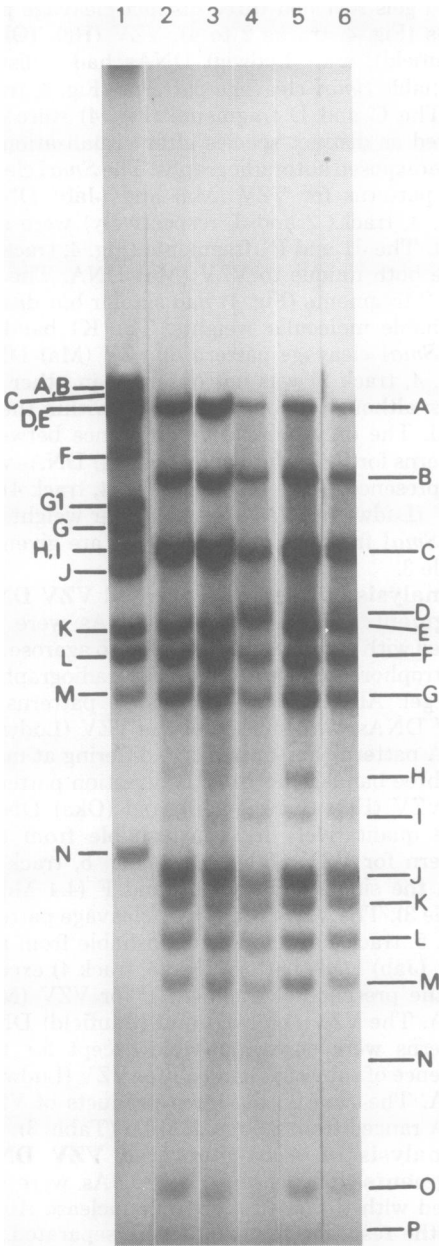

FIG. 3. *Autoradiographs showing the HindIII digestion patterns of VZV DNAs. ^{32}P-labeled VZV DNAs were cleaved with HindIII, and the resulting fragments were separated by agarose gel electrophoresis. Autoradiography of the gel was performed. Track 1 is the standard: HSV-1 (KOS) DNA cleaved by HindIII (22, 28). Selected VZV isolates are: (track 2) VZV (Ma) DNA; (track 3) VZV (Rc) DNA; (track 4) VZV (Oka) DNA; (track 5) VZV (Ludwig) DNA; (track 6) VZV (Jab) DNA.*

TABLE 3. *Molecular weights of VZV DNA fragments generated by restriction enzyme digestion*

Fragment designation	Mol wt (Mdal)[a]			
	*Eco*RI	*Hin*dIII	*Sma*I	*Bam*HI
A	11.0	13	29	8.8
B	10.0	9.4	9.7	6.0
C	9.0	7.4	7.7[b]	5.3
D	8.1	6.2	7.7[b]	4.9
E	7.9	5.8	5.2	4.7
F	5.9	5.3	4.4	4.4
G	5.6	4.7	3.3	3.8
H	5.0	3.7	2.6	3.4
I	4.6	3.3	2.1	2.6
J	3.4	2.6	1.6	1.9
K	2.9	2.5	1.4	1.8
L	2.7	2.2	1.2	1.6
M	1.0	1.9	1.15	1.3
N	0.58	1.5	0.9	1.2
O	0.50	1.1	0.81	1.1
P	0.39	0.9	0.64	1.0
Q	NP[c]	NP	0.55	0.92
R	NP	NP	0.46	0.85
S	NP	NP	0.42	0.80
T	NP	NP	0.38	NP

[a] Molecular weights were calculated as described in the legend to Table 2.

[b] Because bands C and D of the *Sma*I digestion pattern were very close together, only an average molecular weight could be determined.

[c] NP, Not present.

sures revealed the same broad bands. A likely explanation is that the broad bands are multiple overlapping bands due to the presence of a large number of *Ava*I cleavage sites on VZV DNA.

DISCUSSION

VZV is propagated by serial passage of trypsinized, infected cells mixed with uninfected cells. Infectious cell-free VZV is absent in these VZV-infected cultures. Plaque purification to eliminate possible defective virus is not possible at present. Evaluation of the buoyant density results and the restriction endonuclease cleavage patterns for VZV DNA must be prefaced with an awareness that some unknown portion of the VZV population may contain defective DNA.

Synthesis of defective herpesvirus DNA after serial, undiluted passage of virus has been reported for several herpesviruses: pseudorabies virus (2), equine herpesvirus (5), *Herpesvirus saimiri* (7), and HSV (4, 8, 10, 16, 27). Defective HSV DNA populations can have a higher buoyant density than wild-type HSV DNA (4). Ben-Porat et al. (2) have described a population of defective pseudorabies virus DNA that has a lower buoyant density than wild-type DNA. Dis-

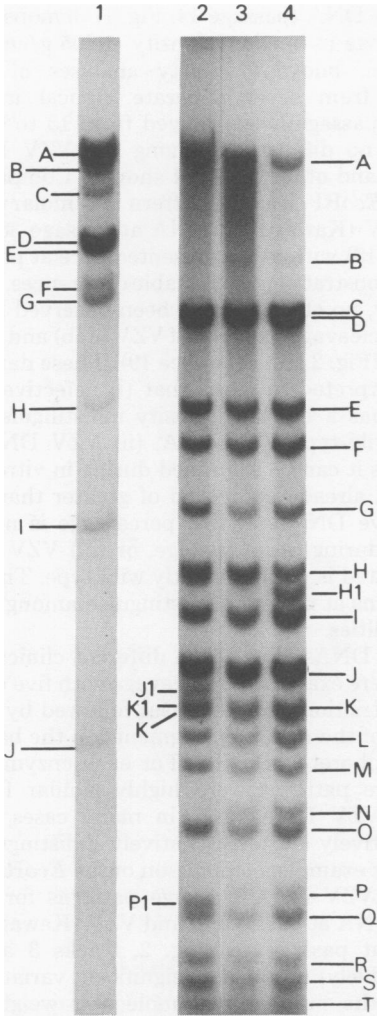

FIG. 4. *Autoradiographs showing the SmaI digestion patterns of VZV DNAs. SmaI cleavage and analysis of seven VZV [^{32}P]DNAs were conducted as described in the legend to Fig. 2. Representative SmaI cleavage patterns for VZV DNAs are: (track 2) VZV (Ma) DNA; (track 3) VZV (Jab) DNA; (track 4) VZV (Ludwig) DNA. The molecular weight standards were produced by EcoRI cleavage of HSV-2 (333) [^{32}P]-DNA (track 1) (11, 23).*

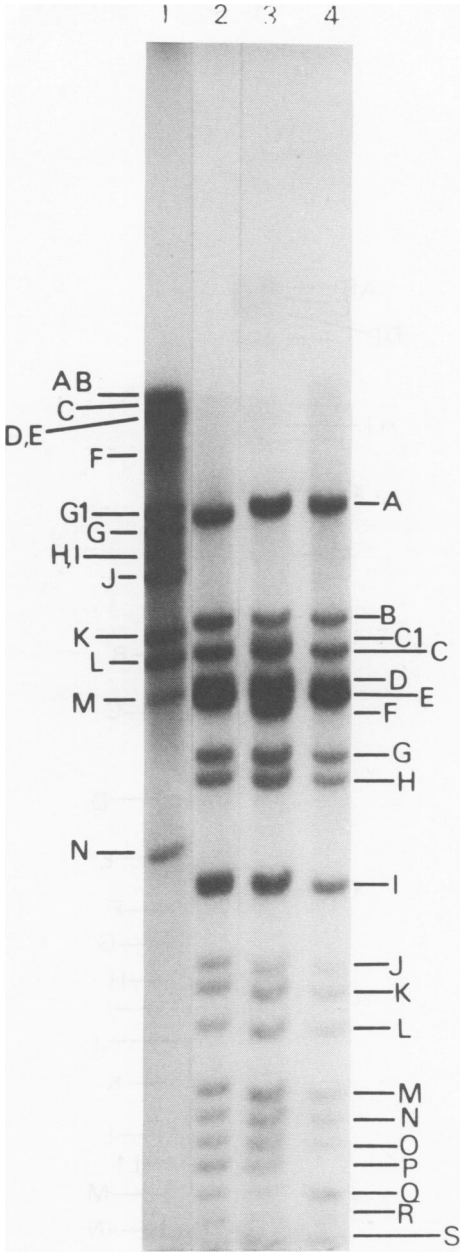

FIG. 5. *Autoradiographs showing the BamHI digestion pattern of VZV DNAs. The BamHI cleavage and analysis of ^{32}P-labeled VZV DNAs were conducted as described in the legend to Fig. 2. Representative BamHI cleavage patterns for VZV DNAs are: (track 2) VZV (Ma) DNA; (track 3) VZV (Ludwig) DNA; (track 4) VZV (Jab) DNA. HindIII digestion of HSV-1 (KOS) DNA generated the molecular weight standards (track 1) (22, 28).*

crete DNA regions of low-passage-derived herpesvirus DNA can be tandemly repeated in defective DNA molecules (2, 9, 16). Comparison of restriction endonuclease cleavage patterns from low-passage and high-passage (defective) HSV DNA revealed major changes in the cleavage patterns of defective HSV DNA (11, 16).

If VZV propagation is analogous to HSV propagation, then accumulation of defective VZV

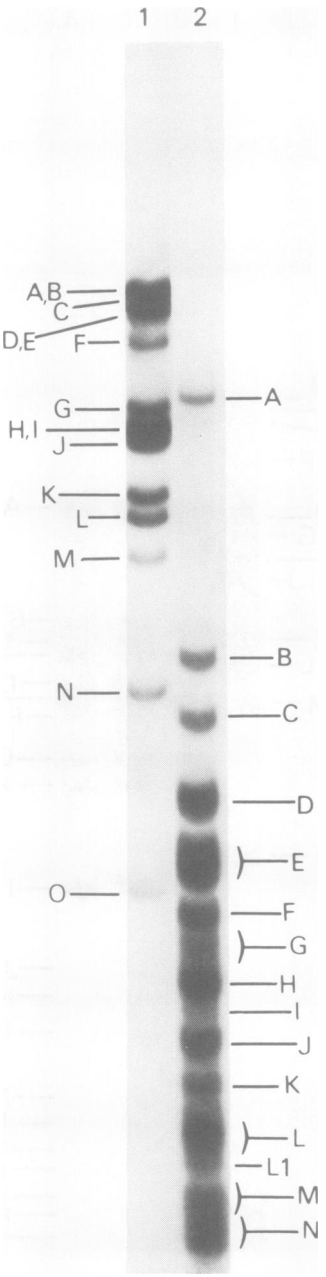

FIG. 6. *Autoradiograph of VZV (Ludwig) [^{32}P]-DNA after cleavage with AvaI and gel electrophoresis. Track 1 is the standard: HSV-1 (Patton) DNA digested by HindIII (22, 28). The AvaI cleavage pattern of VZV (Ludwig) DNA (track 2) is representative of the AvaI cleavage profiles for the DNAs from all seven clinical VZV isolates.*

DNA may occur during the course of serial VZV passage. Comparison of the buoyant density of early passage VZV (Jab) DNA (passage 0 to 5; reference 13) with the buoyant density of later-passage DNA (passage 14; Fig. 1) demonstrates no change in buoyant density (1.705 g/cm^3). In addition, buoyant density analyses of VZV DNAs from seven separate clinical isolates whose passage levels ranged from 13 to 48 revealed no differences among the VZV DNAs (Fig. 1 and other data not shown). Comparison of the *Eco*RI cleavage pattern and molar yields for VZV (Kawaguchi) DNA at passage 30 (reference 19) with those presented here at passage 47 demonstrated no detectable differences. Analogously, no changes have been observed in the *Eco*RI cleavage patterns of VZV (Jab) and (Oka) DNAs (Fig. 2 and reference 19). These data can be interpreted to mean that (i) defective VZV DNA has a buoyant density indistinguishable from wild-type VZV DNA, (ii) VZV DNA, as early as it can be examined during in vitro passage, is already composed of greater than 90% defective DNA and this percentage is not reduced during serial passage, or (iii) VZV DNA as isolated is predominantly wild type. There is no means at present to distinguish among these possibilities.

VZV DNAs from seven different clinical isolates were examined by cleavage with five different restriction endonucleases followed by separation of the resulting fragments on the basis of electrophoretic mobility. For each enzyme, the cleavage patterns were highly similar for all seven VZV DNAs and, in many cases, were qualitatively and quantitatively indistinguishable. For example, comparison of the *Eco*RI-generated VZV DNA cleavage patterns for VZV (Ma) DNA at passage 10 and VZV (Kawaguchi) DNA at passage 48 (Fig. 2, tracks 3 and 4, respectively) revealed no significant variation in either the number and molecular weights of fragments or in the relative molar yields of comparable fragments (Table 2). The *Eco*RI cleavage pattern for VZV (Rc) DNA (Fig. 2, track 2) demonstrated a 25-Mdal fragment (A1) which was absent in the patterns for all other isolates (Fig. 2, tracks 3 to 7). The B and E fragments (10 and 7.9 Mdal, respectively) were absent in the VZV (Rc) DNA cleavage pattern. The A1 fragment could theoretically be the sum of the B and E fragments (within experimental error), and, therefore, the presence of fragment A1 could be accounted for by a single base change. As a second example, the *Hin*dIII cleavage patterns of VZV DNA (Fig. 3) were very similar, supporting our previous observations (19). The only qualitative differences among the *Hin*dIII cleavage patterns were the additional presence of a single DNA fragment (band D; 6.2 Mdal) in the VZV (Ludwig), (Oka), and (Jab) DNA patterns and the absence of band E in the VZV (Oka) DNA pattern (Fig. 3, track 4). As a final example, *Ava*I digestion of the seven VZV DNAs

produced fragment patterns which were qualitatively indistinguishable (Fig. 6, track 2). We originally chose *Ava*I to evaluate the VZV DNAs for possible differences attributable to the presence of 5-methylcytosine (3). However, no differences were observed.

In summary, the two major conclusions from our data are as follows. (i) There was no significant difference in the CsCl buoyant density of VZV DNA among different clinical isolates. The slight differences observed earlier (13) are now attributed to isotope effect. (ii) The restriction endonuclease cleavage patterns presented here for the DNAs from seven clinical VZV isolates exhibited a large degree of homogeneity among isolates for each specific enzyme. The cleavage patterns among VZV DNAs studied thus far have not shown the variability demonstrated among HSV DNAs (11, 23).

ACKNOWLEDGMENTS

We thank L. Rasmussen, M. Takahashi, and R. Tenser for generously providing us with VZV isolates.

This work was supported by Public Health Service contract N01-CP-53516 within the Virus Cancer Program of the National Cancer Institute and by grants CA 16498 and CA 18450 awarded by the National Cancer Institute. R. W. Hyman is the recipient of a Faculty Research Award from the American Cancer Society (FRA-158).

LITERATURE CITED

1. **Asano, Y., T. Yazaki, T. Miyata, H. Nakayama, S. Hirose, S. Ito, E. Tanaka, S. Isomura, S. Suzuki, and M. Takahashi.** 1975. Application of a live attenuated varicella vaccine to hospitalized children and its protective effect on spread of varicella infection. Biken J. **18**:35–40.
2. **Ben-Porat, T., J. M. Demarchi, and A. S. Kaplan.** 1974. Characterization of defective interfering viral particles present in a population of pseudorabies virions. Virology **61**:29–37.
3. **Bird, A. P., and E. M. Southern.** 1978. Use of restriction enzymes to study eukaryotic DNA methylation. 1. The methylation pattern in ribosomal DNA from *Xenopus laevis*. J. Mol. Biol. **118**:27–47.
4. **Bronson, D. L., G. R. Dreesman, N. Biswal, and M. Benyesh-Melnick.** 1973. Defective virions of herpes simplex viruses. Intervirology **1**:141–153.
5. **Campbell, D. E., M. C. Kemp, M. L. Perdue, C. C. Randall, and G. A. Gentry.** 1976. Equine herpesvirus *in vivo*: cyclic production of a DNA density variant with repetitive sequence. Virology **69**:737–750.
6. **Cassai, E., and S. Bachenheimer.** 1973. Effect of isotope label on buoyant density determinations of viral DNA in the preparative ultracentrifuge. J. Virol. **11**:610–613.
7. **Fleckenstein, B., G. W. Bornkamm, and H. Ludwig.** 1975. Repetitive sequences in complete and defective genomes of *Herpesvirus saimiri*. J. Virol. **15**:398–406.
8. **Frenkel, N., R. J. Jacob, R. W. Honess, G. S. Hayward, H. Locker, and B. Roizman.** 1975. Anatomy of herpes simplex virus DNA. III. Characterization of defective DNA molecules and biological properties of virus populations containing them. J. Virol. **16**:153–167.
9. **Frenkel, N., H. Locker, W. Batterson, G. S. Hayward, and B. Roizman.** 1976. Anatomy of herpes simplex virus DNA. VI. Defective DNA originates from the S component. J. Virol. **20**:527–531.
10. **Graham, B. J., Z. Bengali, and G. F. Vande Woude.** 1978. Physical map of the origin of defective DNA in herpes simplex virus type 1 DNA. J. Virol. **25**:878–887.
11. **Hayward, G. S., N. Frenkel, and B. Roizman.** 1975. Anatomy of herpes simplex virus DNA: strain differences and heterogeneity in the locations of restriction endonuclease cleavage sites. Proc. Natl. Acad. Sci. U.S.A. **72**:1768–1772.
12. **Hirt, B.** 1967. Selective extraction of polyoma DNA from infected mouse cell cultures. J. Mol. Biol. **26**:365–369.
13. **Iltis, J. P., J. E. Oakes, R. W. Hyman, and F. Rapp.** 1977. Comparison of the DNAs of varicella-zoster viruses isolated from clinical cases of varicella and herpes zoster. Virology **82**:345–352.
14. **Kieff, E. D., S. L. Bachenheimer, and B. Roizman.** 1971. Size, composition and structure of the DNA of subtypes 1 and 2 of herpes simplex viruses. J. Virol. **8**: 125–132.
15. **Kudler, L., and R. W. Hyman.** 1979. Exonuclease III digestion of herpes simplex virus DNA. Virology **92**:68–81.
16. **Locker, H., and N. Frenkel.** 1979. Structure and origin of defective genomes contained in serially passaged herpes simplex virus type 1 (Justin). J. Virol. **29**:1065–1077.
17. **Ludwig, H., H. G. Haines, N. Biswal, and M. Benyesh-Melnick.** 1972. The characterization of varicella zoster virus DNA. J. Gen. Virol. **14**:111–114.
18. **McDonell, M., M. Simon, and F. W. Studier.** 1977. Analysis of restriction fragments of T7 DNA and determination of molecular weights by electrophoresis in neutral and alkaline gels. J. Mol. Biol. **110**:119–146.
19. **Oakes, J. E., J. P. Iltis, R. W. Hyman, and F. Rapp.** 1977. Analysis by restriction enzyme cleavage of human varicella-zoster virus DNAs. Virology **82**:353–361.
20. **Rapp, F., J. P. Iltis, J. E. Oakes, and R. W. Hyman.** 1977. A novel approach to study the DNA of herpes zoster virus. Intervirology **8**:272–280.
21. **Sharp, P. A., B. Sugden, and J. Sambrook.** 1973. Detection of two restriction endonuclease activities in *Haemophilus parainfluenzae* using analytical agarose-ethidium bromide electrophoresis. Biochemistry **12**: 3055–3063.
22. **Skare, J., and W. C. Summers.** 1977. Structure and function of herpesvirus genomes. II. *Eco*RI, *Xba*I and *Hin*dIII exonuclease cleavage sites on herpes simplex virus type 1 DNA. Virology **76**:581–596.
23. **Skare, J., W. Summers, and W. C. Summers.** 1975. Structure and function of herpesvirus genomes. I. Comparison of five HSV-1 and two HSV-2 strains by cleavage of their DNA with *Eco*R-1 restriction endonuclease. J. Virol. **15**:726–732.
24. **Swanstrom, R., and P. Shank.** 1978. X-ray intensifying screens greatly enhance the detection by autoradiography of the radioactive isotopes ^{32}P and ^{125}I. Anal. Biochem. **86**:184–192.
25. **Takahashi, M., Y. Okuno, T. Otsuka, J. Osame, A. Takamizawa, T. Sasada, and T. Kubo.** 1975. Development of a live attenuated varicella vaccine. Biken J. **18**:25–33.
26. **Taylor-Robinson, D., and A. E. Caunt.** 1972. The varicella virus. Virol. Monogr. **12**:4–88.
27. **Wagner, M., J. Skare, and W. C. Summers.** 1974. Analysis of DNA of defective herpes simplex virus type 1 by restriction endonuclease cleavage and nucleic acid hybridization. Cold Spring Harbor Symp. Quant. Biol. **39**:683–686.
28. **Wilkie, N.** 1976. Physical maps for herpes simplex virus type 1 DNA for restriction endonucleases *Hin*dIII, *Hpa*I and *Xba*I. J. Virol. **20**:222–233.